

## Supplementary Information

### A divergent strategy for the synthesis of redox-active verdazyl radical polymers

François Magnan<sup>a,b</sup>, Jasveer S. Dhindsa<sup>a,b</sup>, Michael Anghel,<sup>a,b</sup> Paul Bazylewski<sup>b,c</sup>,

Giovanni Fanchini<sup>a,b,c\*</sup>, and Joe B. Gilroy<sup>a,b\*</sup>

*<sup>a</sup>Department of Chemistry, The University of Western Ontario, London, Ontario, Canada, N6A 5B7. <sup>b</sup>The Centre for Advanced Materials and Biomaterials Research (CAMBR), The University of Western Ontario, London, ON, Canada, N6A 5B7. <sup>c</sup>Department of Physics and Astronomy, The University of Western Ontario, London, Ontario, Canada, N6A 3K7.*

*Correspondence to: G. Fanchini (E-mail: [gfanchin@uwo.ca](mailto:gfanchin@uwo.ca)) and J. B. Gilroy (E-mail: [joe.gilroy@uwo.ca](mailto:joe.gilroy@uwo.ca))*

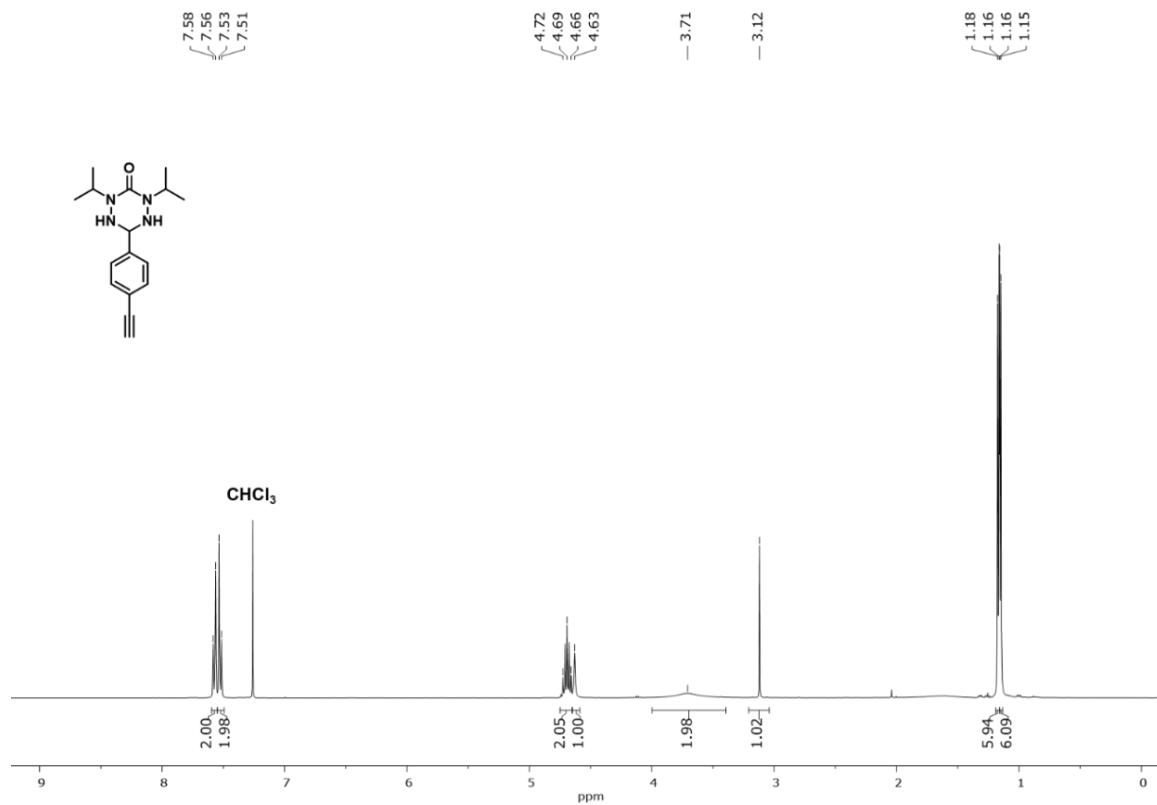


**Fig. S1**  $^1\text{H}$  NMR spectrum of tetrazane **2** in  $\text{CDCl}_3$ .

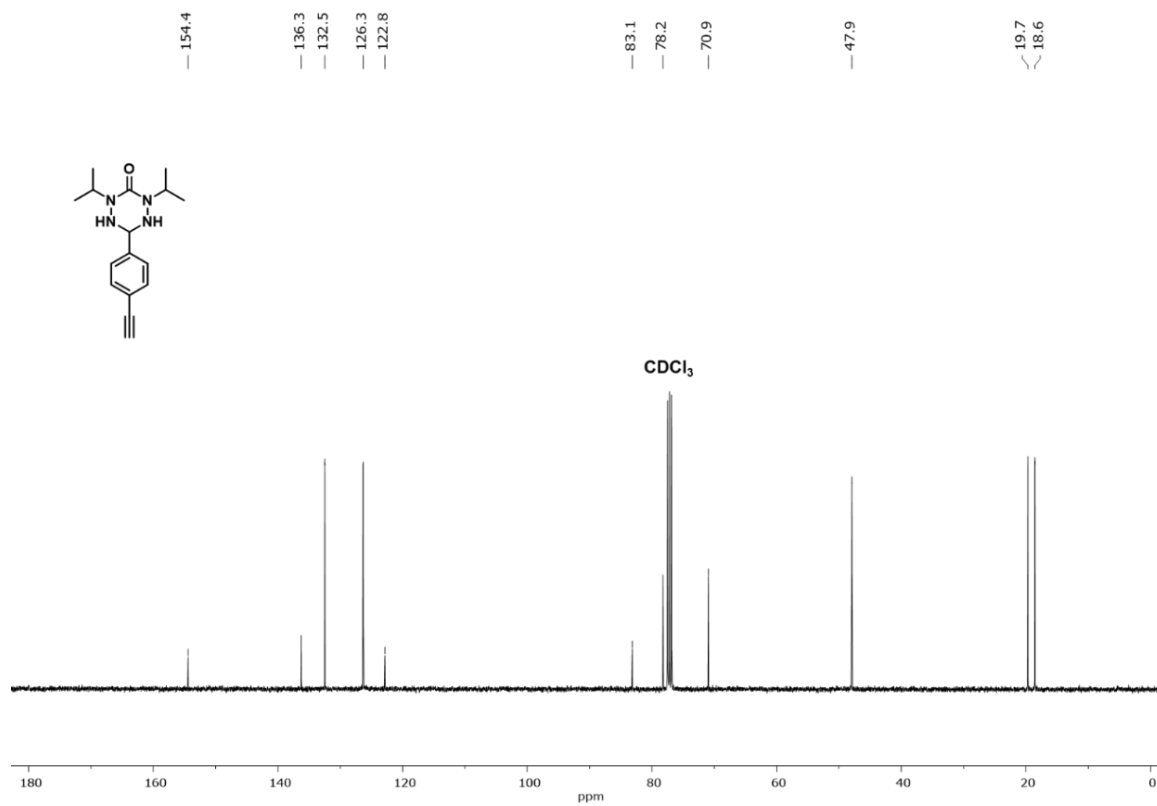


**Fig. S2**  $^{13}\text{C}\{^1\text{H}\}$  NMR spectrum of tetrazane **2** in  $\text{CDCl}_3$ .

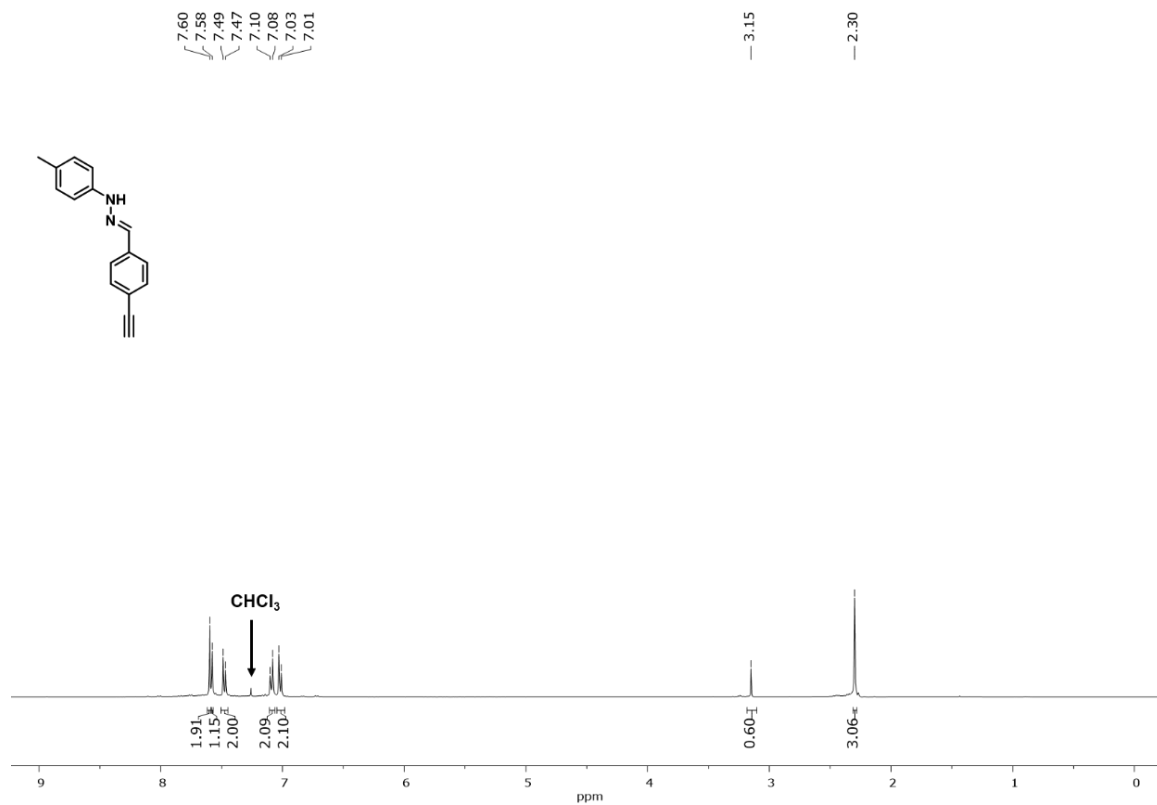


**Fig. S3**  $^1\text{H}$  NMR spectrum of hydrazone **4** in  $\text{CDCl}_3$ .

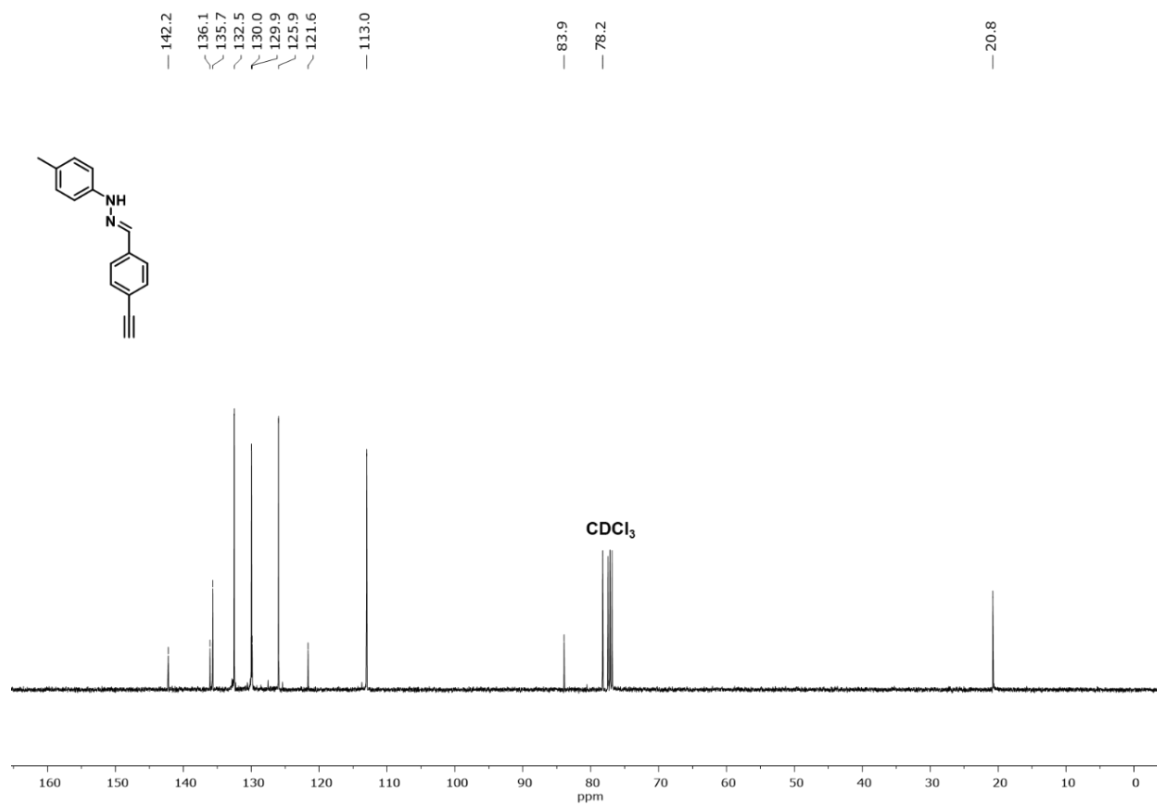


**Fig. S4**  $^{13}\text{C}\{^1\text{H}\}$  NMR spectrum of hydrazone **4** in  $\text{CDCl}_3$ .

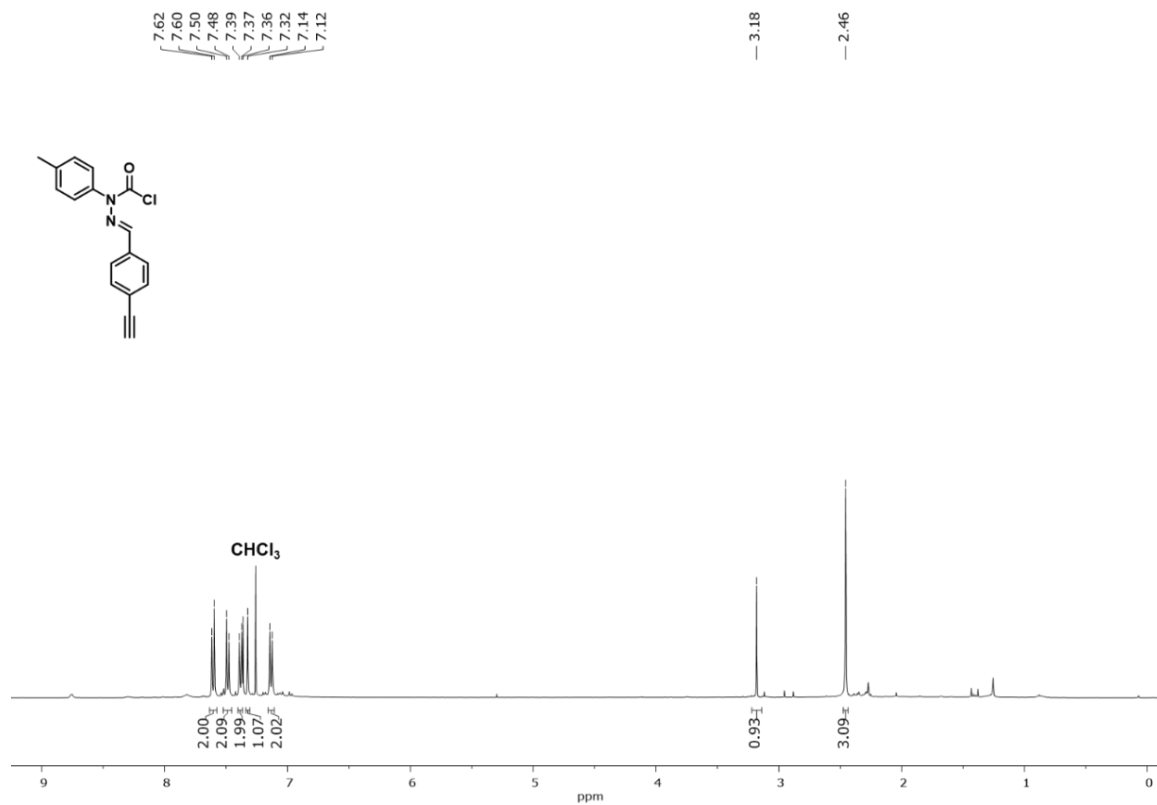


**Fig. S5**  $^1\text{H}$  NMR spectrum of chloroformylhydrazone **5** in  $\text{CDCl}_3$ .

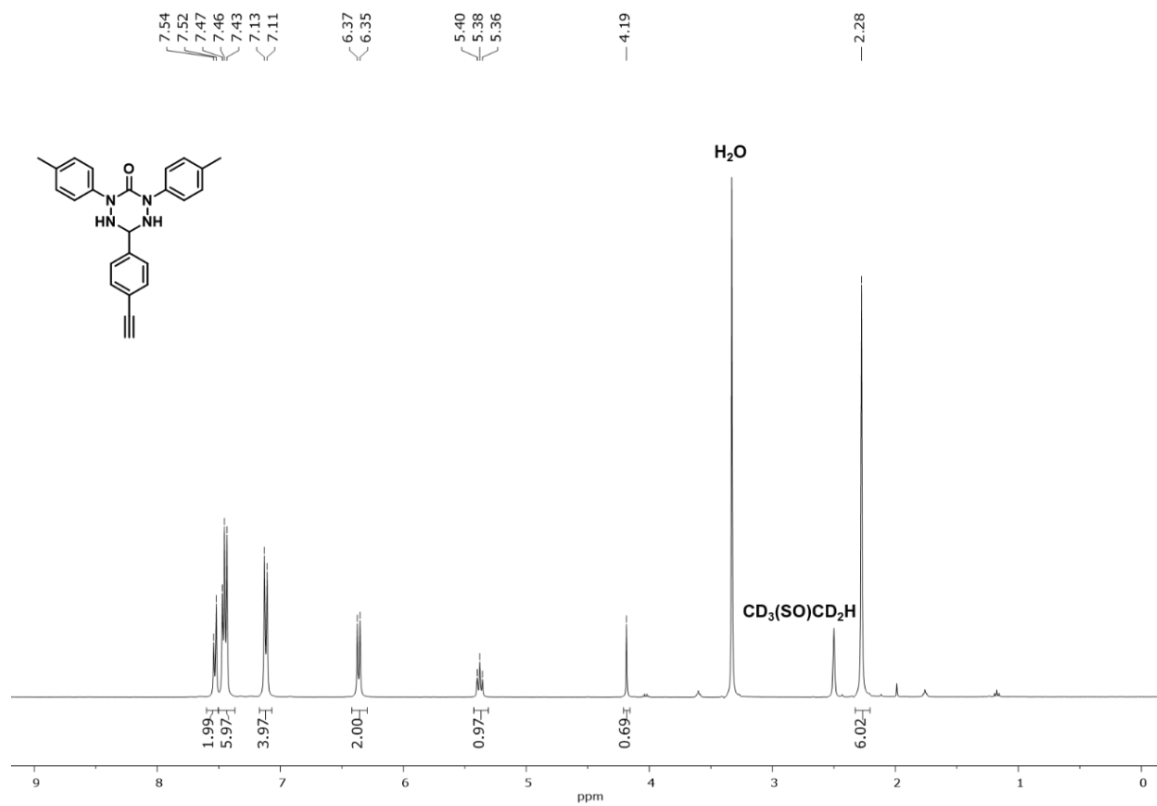


**Fig. S6**  $^1\text{H}$  NMR spectrum of tetrazane **6** in  $\text{DMSO}-d_6$ .

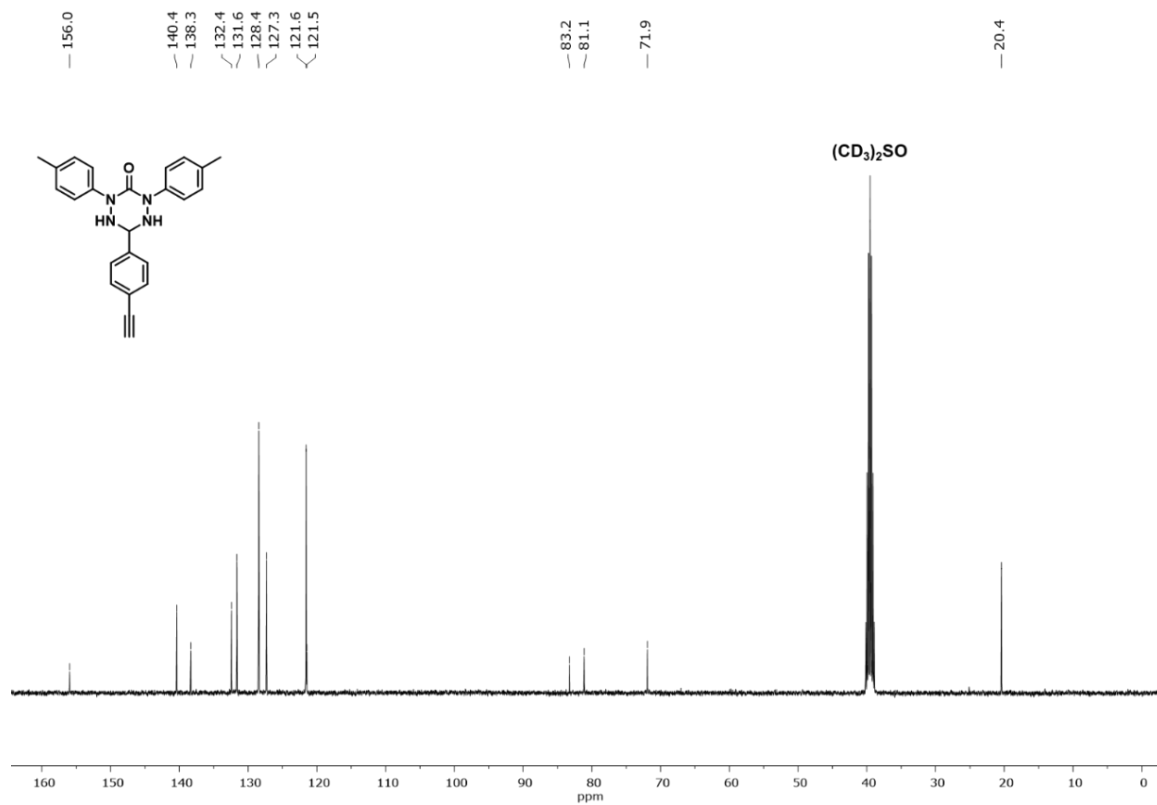


**Fig. S7**  $^{13}\text{C}\{^1\text{H}\}$  NMR spectrum of tetrazane **6** in  $\text{DMSO-}d_6$ .

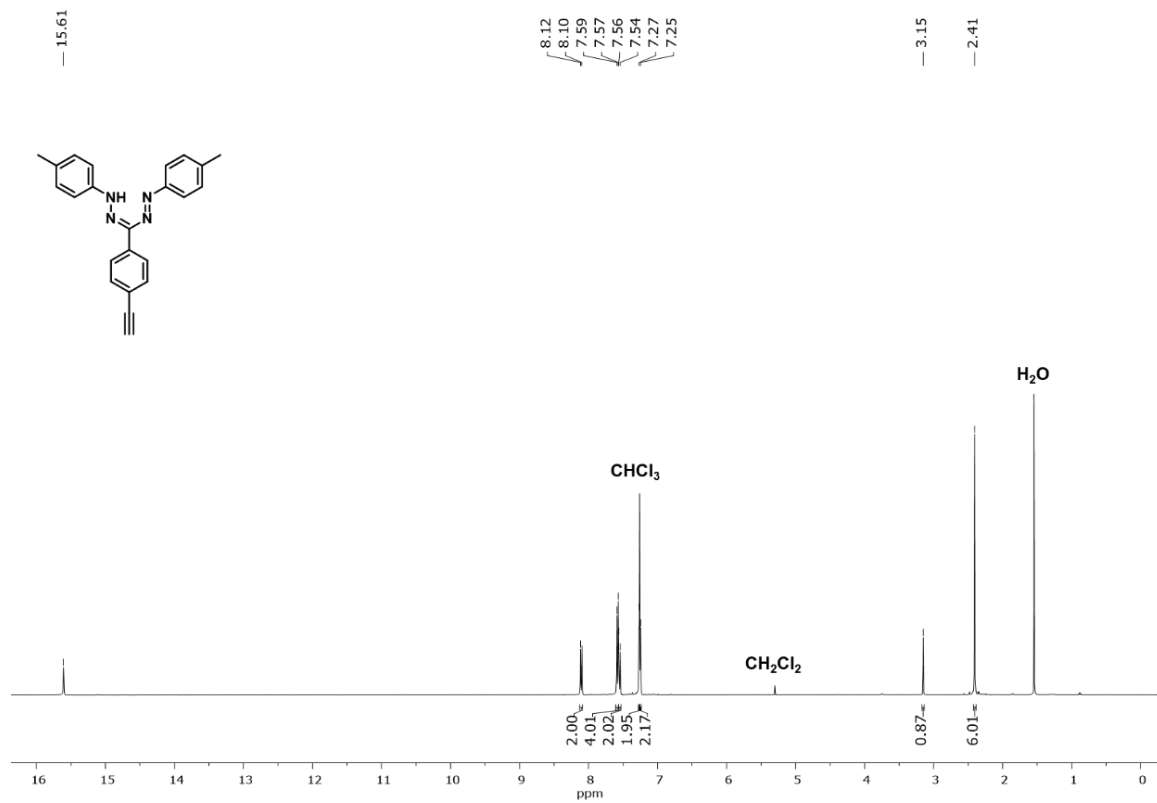


**Fig. S8**  $^1\text{H}$  NMR spectrum of formazan **8** in  $\text{CDCl}_3$ .

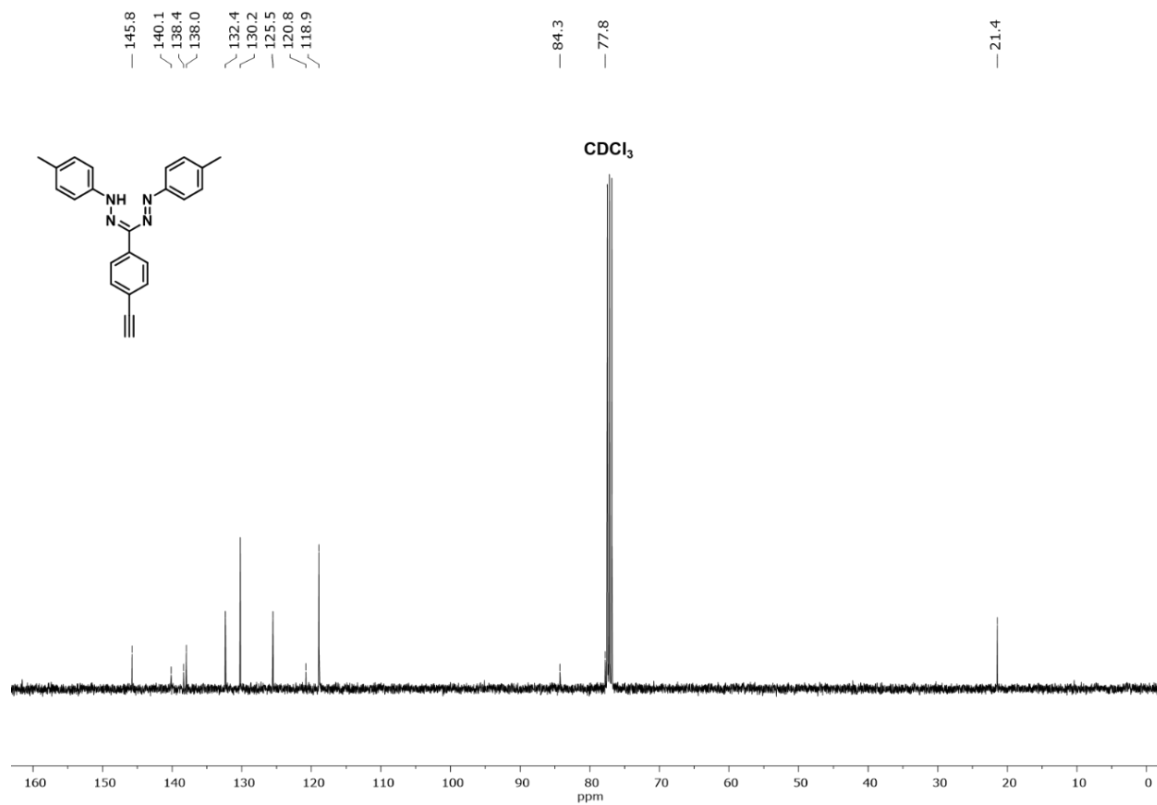


**Fig. S9**  $^{13}\text{C}\{^1\text{H}\}$  NMR spectrum of formazan **8** in  $\text{CDCl}_3$ .

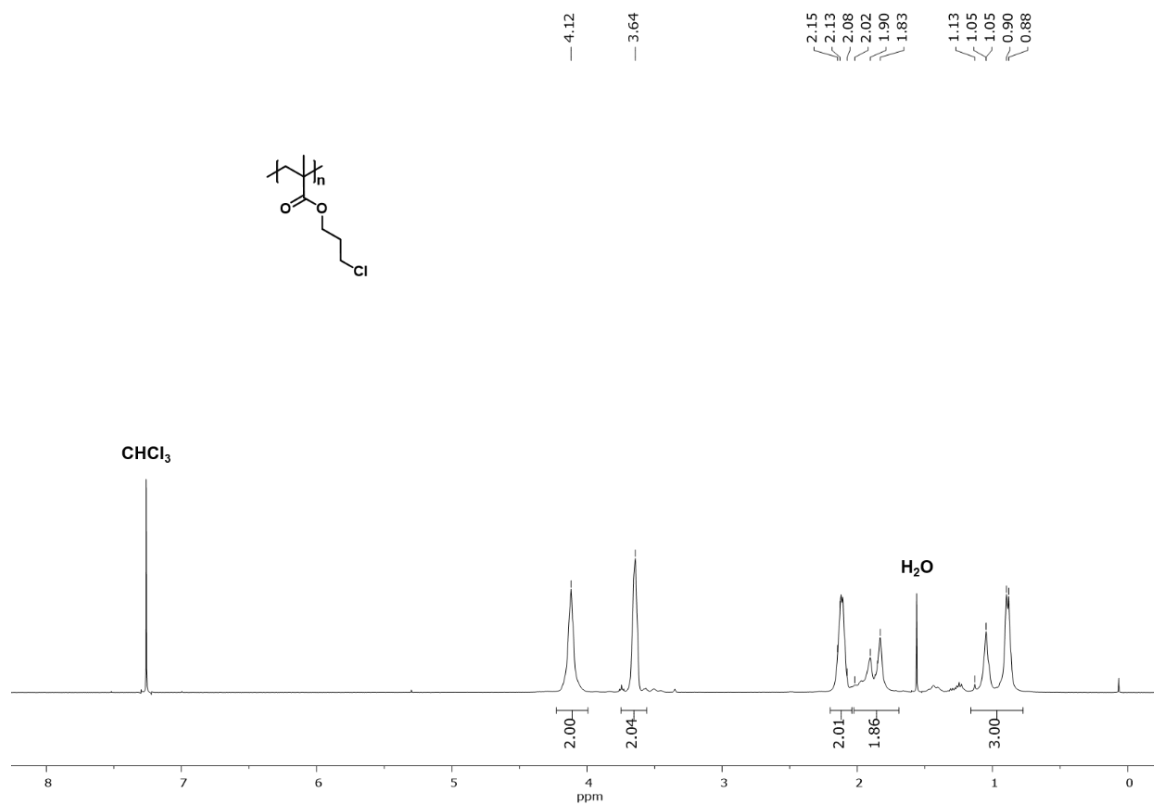


**Fig. S10**  $^1\text{H}$  NMR spectrum of polymer **Cl-P** in  $\text{CDCl}_3$ .

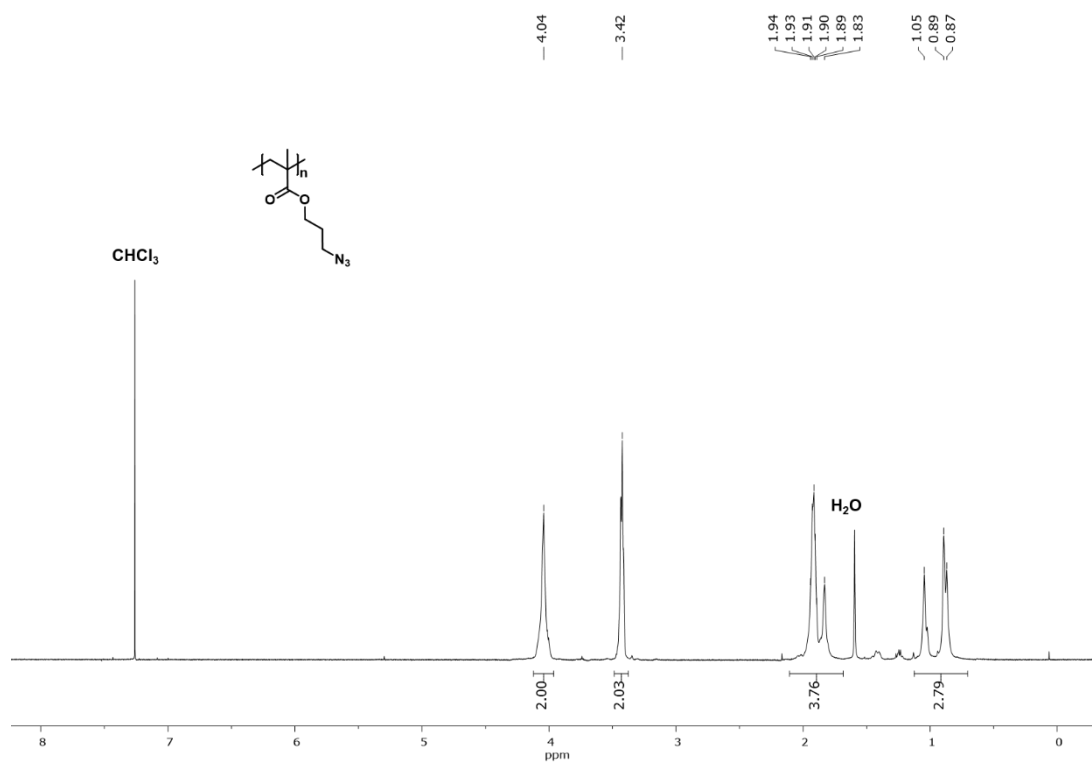


**Fig. S11**  $^1\text{H}$  NMR spectrum of polymer  $\text{N}_3\text{-P}$  in  $\text{CDCl}_3$ .

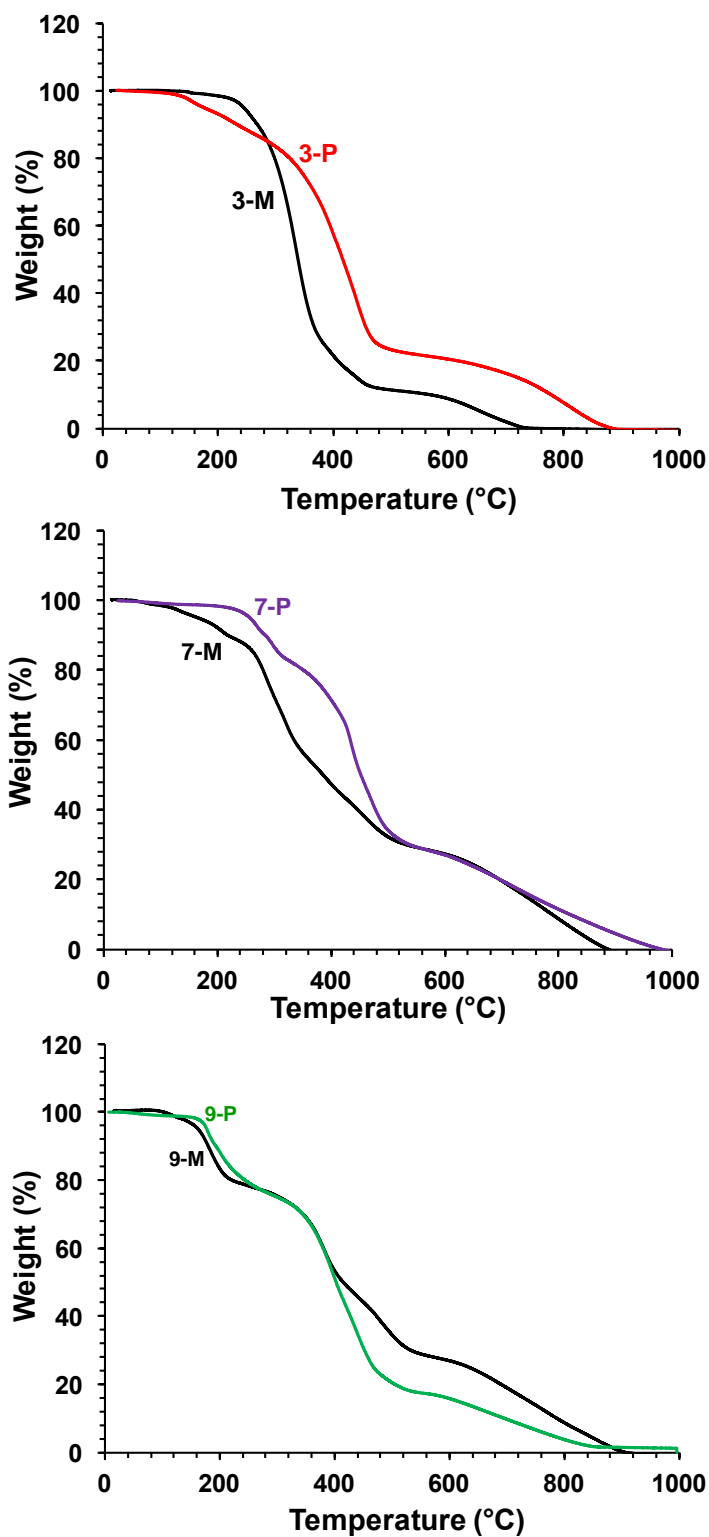


**Fig. S12** TGA data for radical monomers **3-M**, **7-M**, and **9-M** and radical polymers **3-P**, **7-P**, and **9-P** collected under an atmosphere of N<sub>2</sub>.



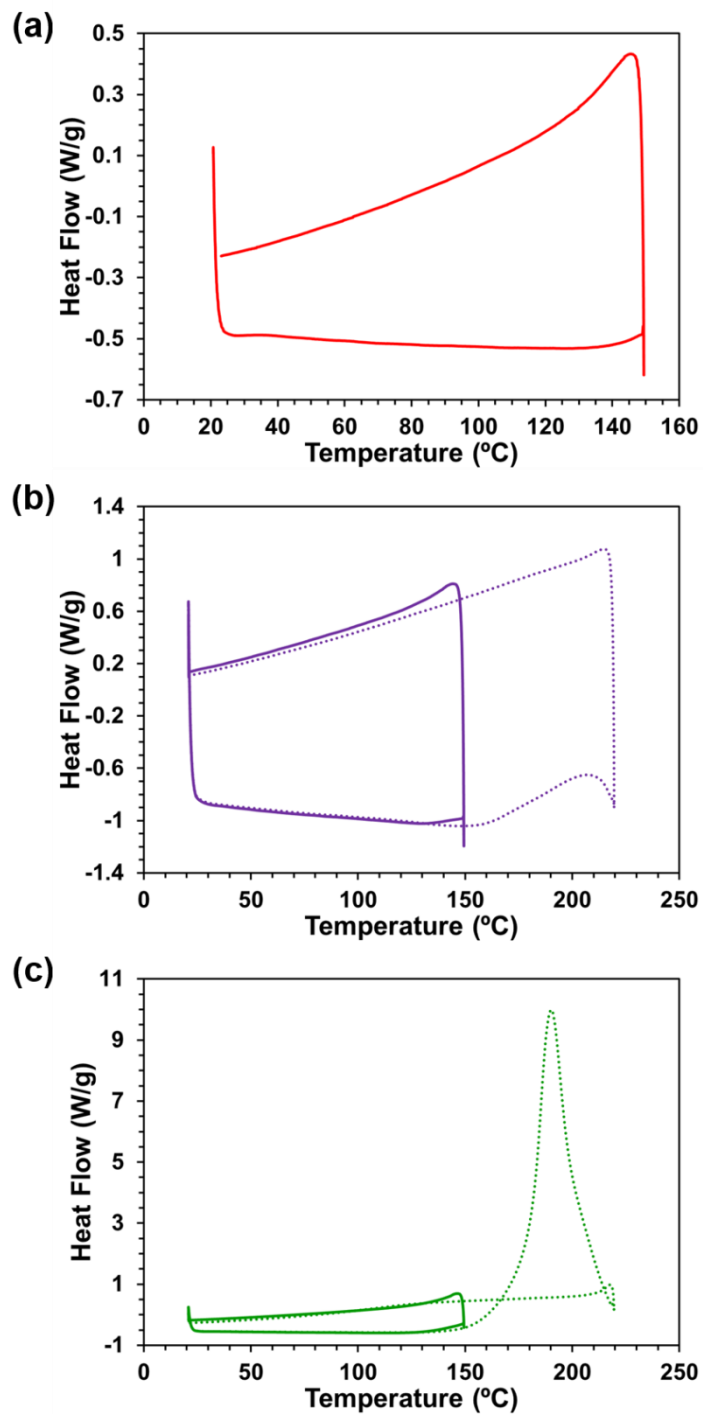


**Fig. S13** DSC data for polymers (a) **3-P**, (b) **7-P**, and (c) **9-P** collected between 20 and 150 °C at a scan rate of 10 °C min<sup>-1</sup>. Dotted lines in (b) and (c) show data collected for the same sample (3<sup>rd</sup> cycle) with heating and cooling cycle between 20 and 220 °C at a scan rate of 10 °C min<sup>-1</sup>.

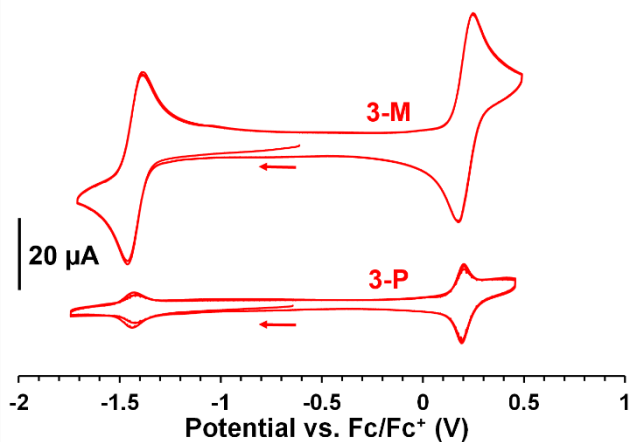


**Fig. S14** Cyclic voltammograms of model radical **3-M** and polymer **3-P** collected upon cycling. Experiments were conducted at a scan rate of  $250 \text{ mV s}^{-1}$  in degassed mixtures of 3:1 v/v  $\text{CH}_2\text{Cl}_2/\text{CH}_3\text{CN}$  containing approximately 1 mM of analyte and 0.1 M  $[\text{nBu}_4\text{N}][\text{PF}_6]$  as the supporting electrolyte.

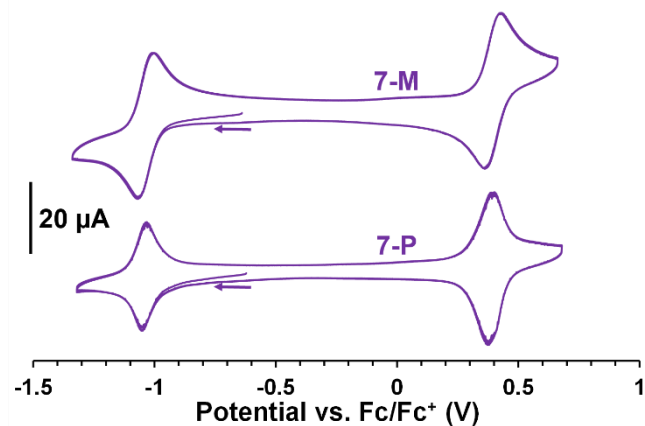


**Fig. S15** Cyclic voltammograms of model radical **7-M** and polymer **7-P** collected upon cycling. Experiments were conducted at a scan rate of  $250 \text{ mV s}^{-1}$  in degassed mixtures of 3:1 v/v  $\text{CH}_2\text{Cl}_2/\text{CH}_3\text{CN}$  containing approximately 1 mM of analyte and 0.1 M  $[\text{nBu}_4\text{N}][\text{PF}_6]$  as the supporting electrolyte.

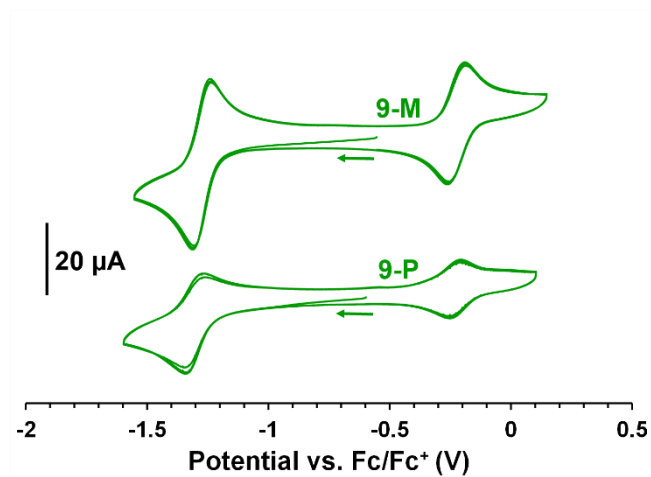


**Fig. S16** Cyclic voltammograms of model radical **9-M** and polymer **9-P** collected upon cycling. Experiments were conducted at a scan rate of  $250 \text{ mV s}^{-1}$  in degassed mixtures of 3:1 v/v  $\text{CH}_2\text{Cl}_2/\text{CH}_3\text{CN}$  containing approximately 1 mM of analyte and 0.1 M  $[\text{nBu}_4\text{N}][\text{PF}_6]$  as the supporting electrolyte.